

## Neutron depolarization in a reentrant spin-glass system: Amorphous Fe-Mn

I. Mirebeau

*Laboratoire Léon Brillouin, Centre d'Etudes Nucléaires de Saclay, 91191 Gif-sur-Yvette CEDEX, France*

S. Itoh

*Department of Physics, Tohoku University, Sendai 980, Japan*

S. Mitsuda

*Institute for Solid State Physics, University of Tokyo, Roppongi Minato Ku, Tokyo 106, Japan*

T. Watanabe and Y. Endoh

*Department of Physics, Tohoku University, Sendai 980, Japan*

M. Hennion and R. Papoular

*Laboratoire Léon Brillouin, Centre d'Etudes Nucléaires de Saclay, 91191 Gif-sur-Yvette CEDEX, France*

(Received 19 October 1989; revised manuscript received 1 February 1990)

Polarization analysis of the transmitted beam has been performed in a reentrant spin-glass system  $(\text{Fe}_{1-x}\text{Mn}_x)_{75}\text{P}_{16}\text{B}_6\text{Al}_3$  for several concentrations  $x$  starting from the true ferromagnet to the true spin glass. The influence of some important parameters like the temperature, the sample thickness, the neutron wavelength, and the applied magnetic field, as well as the cooling conditions, has been checked. Large ferromagnetic domains of about  $30\ \mu\text{m}$  size are evident in the nonfrustrated alloy ( $x=0.07$ ). In the weakly frustrated samples ( $0.22 < x < 0.26$ ), smaller domains of about  $4$  to  $6\ \mu\text{m}$  are observed, which persist at low temperature. In the strongly frustrated  $x=0.30$  sample, we observe a decrease of the domain size or of the internal magnetization at low temperature. The results in the weakly frustrated alloys support the coexistence at low temperature of a long-range longitudinal order together with frozen transverse spin components, in good agreement with the mean-field predictions. The limits of the infinite-range mean-field model are shown in the sample close to the critical point.

### I. INTRODUCTION

Reentrant spin glasses (RSG's) can be defined by the existence of a competition between ferromagnetic and antiferromagnetic interactions—with a nonzero value of the mean interaction—associated with a site or bond randomness. The resulting “frustration” yields a very specific phase diagram. With decreasing temperature, the system first undergoes a transition from the paramagnetic to the ferromagnetic (or antiferromagnetic state) at  $T_c$ , then at a lower temperature  $T_f$  “reenters” a magnetic state that resembles the usual spin-glass state. The question to decide whether the reentrant spin-glass state is really a broken-symmetry state or if it differs from the usual spin-glass state has been the subject of many controversies from both theoretical and experimental points of view.

From the theoretical side, several pictures have been proposed. In the mean-field model (MF) developed by Sherrington and Kirkpatrick<sup>1</sup> in the Ising case, then extended by Gabay and Toulouse<sup>2</sup> to the Heisenberg case, two transitions are predicted below  $T_c$ : first a freezing of transverse spin components associated with the occurrence of small irreversibilities, and then at a lower temperature, another transition, reminiscent of the De Almeida–Thouless one in pure spin glasses. In this mod-

el, the low-temperature state consists in a mixed phase, since the long-range longitudinal order still coexists with the frozen transverse spins. The existence of a freezing process is also predicted in the local mean-field approach recently developed by Saslow and Parker.<sup>3</sup> In this latter case, a decrease of the magnetization is predicted at low temperature since the frozen spins progressively tip over the nonfrustrated ones. Finally, in the inhomogeneous picture of the random-field approach (RF) developed by Aeppli *et al.*,<sup>4</sup>  $T_c$  is defined by the percolation of a ferromagnetic cluster that coexists with other small clusters. At low temperature, the random fields induced by the small clusters break the infinite one. Note that the RF model is rather phenomenological since clusters are assumed to produce the random fields necessary to break down the ferromagnetic order, whereas in the MF model the temperature evolution is derived from the exchange interaction only. Roughly speaking, the MF and RF approaches yield opposite predictions concerning the low-temperature state: a long-range longitudinal order and uncorrelated transverse spin components within the MF model, a breakdown of the long-range order associated with a finite correlation length in the RF one.

From an experimental point of view, reentrant spin glasses have been extensively studied since they are observed in a large variety of systems, either ferromagnetic

or antiferromagnetic, crystalline or amorphous, insulating or metallic. The degree of frustration is easily controlled by varying the concentration of the magnetic species and/or the degree of positional disorder with an appropriate heat treatment. However, the experimental results do not easily permit choice between the above-mentioned pictures. Measurements of the hyperfine field indicate a freezing of transverse spin components that favor the MF model. Low-field magnetization data reveal a strong decrease of the magnetization below  $T_f$ , which has been associated with a breakdown of the ordered state within the RF model,<sup>5</sup> while it could be as well interpreted by a blocking of domain walls. At low temperature, the large hysteresis exhibited by the magnetization that depends on the cooling conditions supports the existence of noncollinear spin components which would induce a Dzyaloshinsky-Moriya type of anisotropy as in usual spin glasses. However, these features do not exclude the persistence, at least in the weakly frustrated RSG's, of a longitudinal order within ferromagneticlike domains. This latter conclusion was drawn from extended magnetization measurements in some NiMn,<sup>6</sup> AuFe,<sup>7</sup> and  $\alpha$ -FeMn,<sup>8</sup> alloys with a rather low frustration character, and recently confirmed by a direct observation of the domains with electron microscopy.<sup>9</sup>

In this respect, it is important to perform a systematic study of the long-range scale with variation of the frustration from the "true" ferromagnet or antiferromagnet, to the true spin glass. A study of the spin-glass phase by electron microscopy is difficult because of the lack of magnetic contrast. In principle, a neutron measurement of the magnetic Bragg peak as a function of temperature and magnetic concentration would provide this information since it measures the Fourier transform of the long-range correlations. In the Ising antiferromagnetic system FeMnTiO<sub>3</sub>,<sup>10</sup> recent neutron measurements demonstrated the coexistence of antiferromagnetic and spin-glass ordering and strongly suggested the existence of a phase boundary between mixed and true spin-glass phases. In reentrant ferromagnets, this experiment is extremely difficult since the ferromagnetic Bragg peak coincides with a nuclear one of much larger magnitude, and very few measurements have been performed so far.<sup>11</sup>

We have used the method of polarization analysis to distinguish between the ferromagnetic long-range order (LRO) and the other state of either normal spin glass or reentrant spin glass. In unsaturated ferromagnets, the precession of the neutron spins over a succession of large, randomly distributed, ferromagnetic domains induces an overall depolarization of the incoming polarized neutron beam.<sup>12</sup> The depolarization value of the transmitted intensity depends on the sample thickness, the neutron wavelength, and the field integral over a domain; that is, on the domain size and magnetization. Note that since this particular experiment implies a measurement of the transmitted neutron beam and not of the scattered one, as in a usual diffraction experiment, the measured intensity is not related to the microscopic neutron-spin interaction. It only reflects the precession of the neutron spin over the rather macroscopic scale that corresponds to the mean domain size.

The investigation of the ferromagnetic domains by the means of neutron depolarization was initiated in pure iron by Halpern and Holstein,<sup>12</sup> and extended to three-dimensional polarization by Rekveldt.<sup>13</sup> As shown by Mitsuda and Endoh,<sup>14</sup> the study of the polarization as a function of the neutron wavelength appears to be a very important check of the models commonly developed to analyze the depolarization data. The use of pulsed polychromatic neutrons and of magnetic supermirrors permits measurements of the depolarization in a wide wavelength range of about 3–10 Å. Such measurements were performed in nonfrustrated ferromagnets like Fe<sub>85</sub>Cr<sub>15</sub> alloys.<sup>14</sup> In this case significant differences in the wavelength dependence were observed between the annealed and the quenched sample and were related to an increase of the domain size with annealing.

In reentrant ferromagnets, we expect a strong change of the depolarization value with both temperature and frustration character. No depolarization should be observed when the magnetic disorder occurs on short scales as in the paramagnetic or true spin-glass phase, whereas a strong depolarization is expected in the ferromagnetic state. In some weakly frustrated  $\alpha$ -Fe<sub>1-x</sub>Mn<sub>x</sub> alloys, (0.22 <  $x$  < 0.26) preliminary measurements at fixed wavelength<sup>15,16</sup> strongly suggested the existence of large domains of a few microns' size, which persisted below the freezing temperature  $T_f$ . By contrast a recent depolarization study of a Fe<sub>0.7</sub>Al<sub>0.3</sub> sample was consistent with an inhomogeneous low-temperature state in which small ferromagnetic clusters were imbedded in spin-glasslike regions.<sup>17</sup>

We present here a systematic study of the neutron depolarization in a reentrant spin-glass system  $\alpha$ -Fe<sub>1-x</sub>Mn<sub>x</sub>. The large range of concentration studied (0.07 <  $x$  < 0.41) extends from the nonfrustrated ferromagnet to the true spin glass. For each sample, the polarization was measured as a function of wavelength and temperature. The influence of some important parameters like the sample thickness, the external field strength, the cooling conditions, and the time or history dependent, has been checked. The results have been analyzed using low- and high-field magnetization data obtained on the same samples and compared to the usual random-field and mean-field models. Similar measurements performed on two other systems, Ni<sub>1-x</sub>Mn<sub>x</sub> and Au<sub>1-x</sub>Fe<sub>x</sub> will be published elsewhere.

## II. SAMPLE DESCRIPTION AND CHARACTERIZATION BY MAGNETIZATION MEASUREMENTS

Eight amorphous samples of (Fe<sub>1-x</sub>Mn<sub>x</sub>)<sub>75</sub>P<sub>16</sub>B<sub>6</sub>Al<sub>3</sub> (0.07 <  $x$  < 0.41) have been prepared by the usual wheelbarrow technique by Bigot and Peynot (Centre d'Etudes de Chimie-Metallurgie, Vitry sur Seine). For the neutron experiments the very absorbing <sup>10</sup>B was replaced by isotopic <sup>11</sup>B. The samples were cut in foils of about one square centimeter surface whose thickness varied from 30–70 μm. The foils could be easily piled up in order to change the total sample thickness. The alloys were characterized by means of low-field magnetization measurements (Fig. 1) from which a typical phase diagram

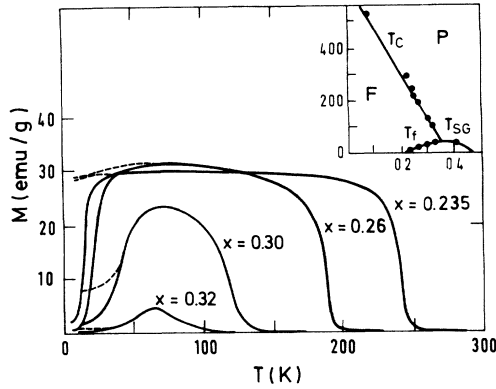


FIG. 1. Low-field magnetization as a function of temperature for several  $a\text{-Fe}_{1-x}\text{Mn}_x$  alloys. The applied field is equal to 20 Oe. The magnetization is measured in the zero-field-cooled state (solid line) and in the field-cooled state (dashed line). Inset: Typical phase diagram deduced from those measurements.

could be obtained (inset of Fig. 1) in good agreement with previous determinations.<sup>5</sup> Depending on concentration, the following temperatures are commonly defined:  $T_c$  and  $T_f$ , respectively, locate the paramagnetic to ferromagnetic transition and the occurrence of *strong* irreversibilities in the system, whereas  $T_{SG}$  corresponds to the paramagnetic to spin-glass (SG) transition. According to the phase diagram, the  $x=0.07$  sample behaves as a usual ferromagnet ( $T_c \sim 525$  K). The  $x=0.22, 0.235, 0.247,$  and  $0.26$  samples correspond to rather weakly frustrated alloys in which the Curie and freezing temperature are far from each other ( $200 < T_c < 300$  K,  $T_f \sim 20$  K). These four samples have been previously studied by small-angle neutron scattering<sup>18</sup> and inelastic scattering.<sup>19</sup> The  $x=0.30$  and  $x=0.32$  samples are very frustrated and close to the tricritical point ( $x=0.35$ ). The  $x=0.41$  sample is a true spin glass.

Note that the onset of strong irreversibilities around  $T_f$  is rather ambiguously defined. In the inset of Fig. 1,  $T_f$  is defined as in the previous measurements of Mannheim *et al.*<sup>5</sup> from the sharp decrease of the low-field magnetization. This temperature roughly corresponds to the temperature below which the coercive field  $H_c$  strongly increases,<sup>7</sup> whereas a maximum is observed in the magnetic viscosity and in the imaginary susceptibility.<sup>20</sup> Weak irreversibilities occur well above  $T_f$ , as shown in Fig. 1, when considering the zero-field-cooled (ZFC) and field-cooled (FC) curves. The occurrence of weak irreversibilities in this temperature range could be related to the freezing of transverse spin components as predicted by the MF theory and discussed in the following.

Magnetization measurements performed in high magnetic field at low temperature ( $H \leq 15$  kOe,  $T \sim 11$  K) (Fig. 2) show for the nonfrustrated or weakly frustrated alloys a sharp increase of the  $M(H)$  curve followed by a technical saturation plateau. This behavior is similar to that observed in conventional ferromagnets in which the magnetic field aligns large domains by suppressing the Bloch walls. However, a residual slope persists at high

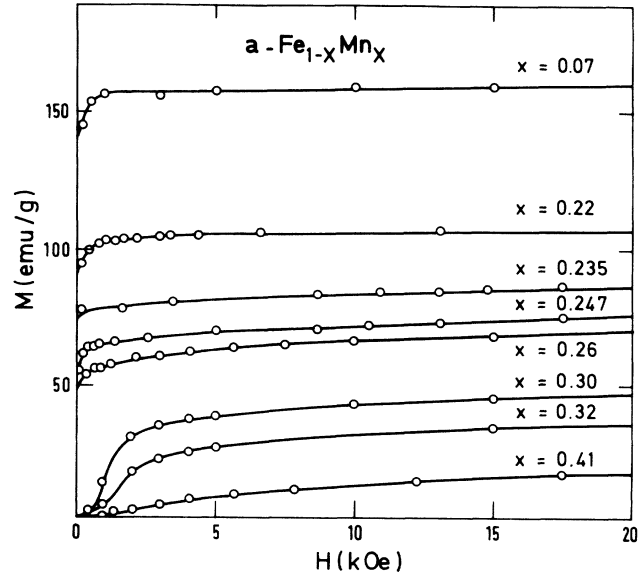


FIG. 2. Magnetization as a function of applied field at low temperature ( $T \sim 11$  K) in the  $a\text{-Fe}_{1-x}\text{Mn}_x$  system.

fields in the  $M(H)$  curve of the frustrated alloys, which suggests the persistence of some disorder within the domains.<sup>21</sup> When increasing the frustration, the knee in the  $M(H)$  curve smears out and it finally disappears in the true spin-glass sample.

### III. EXPERIMENTAL DETAILS

The depolarization measurements were performed at fixed wavelength  $\lambda$  in the Orphee, Institut Max von Laue-Paul Langevin (ILL), and Brookhaven reactors, and as a function of  $\lambda$  in the pulsed neutron source of National Laboratory for High-Energy Physics (KEK) at Tsukuba, during a visit of one of the authors (I.M.). The experimental setup was basically the same for all experiments. A complete description can be found in Refs. 14 and 16. The incident neutron beam was polarized by a magnetic FeCo mirror assembled as curved Sollers slits. The polarization axis, defined as the  $z$  axis, was vertical in most cases. The incomplete beam polarization of the mirror was taken into account by measuring the polarization without the sample or with the sample in the paramagnetic state. The beam transmitted through the sample was analyzed in the  $z$  direction by using a similar magnetic mirror. Thus only the  $z$ - $z$  component of the depolarization matrix was determined. The incident neutron spin state (parallel and antiparallel to the  $z$  axis) was changed using either a Mezei or a Drapkin type of flipper, the flipping efficiency being around 0.98. Magnetic guides were used to maintain the neutron polarization before and after the sample. The magnetic field at the sample position, which was applied along the  $z$  axis, could vary from 0 to a few hundred Oe; most experiments being performed in a low field of 5 or 7 Oe. The sample temperature was varied from 300 to 10 K using a cryogenerator.

A very short wavelength was used on the D5 spectrometer of ILL ( $\lambda=0.8$  Å) and at the Brookhaven reactor ( $\lambda=2.36$  Å). Measurements on the spectrometer PADA

at Orphee ( $\lambda=5 \text{ \AA}$ ) could be performed with a very high value of the incident neutron polarization ( $P_0 \geq 0.97$ ), which allowed measurement of a very low sample depolarization with an excellent precision. Measurements on the neutron spin-echo machine at Orphee were made with a longer wavelength  $\lambda=7 \text{ \AA}$ . In this case, the sample depolarization could be measured in a zero applied field since the earth field was sufficient to guide the neutrons. Finally, most results were obtained on the TOP spectrometer (KEK) where the use of a polychromatic neutron beam permitted measurement of the wavelength dependence of the sample depolarization continuously in the range 3–10  $\text{\AA}$ .

#### IV. RESULTS AND ANALYSIS

Before discussing the experimental results, we briefly summarize the theoretical predictions concerning the polarization in the paramagnetic, ferromagnetic, and spin-glass state. As shown in Refs. 12–14, the polarization is simply related to the Larmor precession of the neutron spin around the magnetic induction  $B$  in the sample. In a paramagnet, the spin fluctuates over a very short-time scale compared to the typical Larmor time for the precession and the neutron spins do not follow the  $B(t)$  variation. In a true spin glass, where the spins are frozen in quasirandom orientations, the spatial variations  $B(r=vt)$  are very short. The neutron spins passing through the sample with velocity  $v$  do not follow the spatial fluctuations of the induction either. Consequently, no depolarization occurs in both cases. In a ferromagnet, the polarization depends on how long the local induction remains in a given direction compared to the Larmor time. Assuming that this direction is unchanged within a domain and changes abruptly from one domain to another, the  $z$ - $z$  component of the polarization is written:<sup>14</sup>

$$P(\lambda) = \left[ 1 - \left\langle \left[ 1 - \langle \cos(cB\delta\lambda) \rangle_\delta \right] \frac{B_x^2 + B_y^2}{B^2} \right\rangle_B \right]^{d/\delta}, \quad (1)$$

where  $\langle \rangle_\delta$  and  $\langle \rangle_B$  are, respectively, the average over the size of domains and orientation of local induction in each domain.  $\delta$  is the mean domain size (cm),  $d$  the sample thickness (cm),  $B$  the local induction in a domain (Oe). The constant  $c(c=gm/2\pi\hbar)$  is equal to  $4.63 \times 10^{-2}$  within these units. For typical values of the magnetic field and neutron wavelength ( $B=5000 \text{ Oe}$ ,  $\lambda=5 \text{ \AA}$ ), the domain size corresponding to one Larmor precession ( $cB\delta\lambda=2\pi$ ) is around  $54 \text{ \mu m}$ . Several simplified expressions of Eq. (1) can be derived in some limiting cases according to the value of  $cB\delta\lambda$ , as shown previously<sup>14</sup> and recorded in the following.

In the  $a\text{-Fe}_{1-x}\text{Mn}_x$  system, Fig. 3 shows qualitatively how the frustration influences the polarization value. The flipping ratio  $R$  and polarization  $P$ , ( $P=[(R-1)/(R+1)]/P_0$ , where  $P_0$  is the polarization without the sample) are plotted versus temperature for several alloys measured in the same experimental conditions ( $H=5 \text{ Oe}$ ,  $\lambda=5 \text{ \AA}$ ). The nonfrustrated  $x=0.07$  sample strongly depolarizes the neutrons in the whole temperature range of experiment. In the reentrant alloys

( $0.22 < x < 0.30$ ), depolarization occurs below the Curie temperature. This depolarization is much more pronounced in the weakly frustrated samples ( $0.22 < x < 0.26$ ) than in the  $x=0.30$  one in which  $P$  remains close to unity. We note that the flipping ratio of this latter sample shows a well-defined minimum. At low temperature it almost recovers its value in the paramagnetic state. Finally, no depolarization is observed in the  $x=0.32$  and  $x=0.41$  samples. In order to get some quantitative information from the depolarization data, we have checked the influence of the other parameters: sample thickness, neutron wavelength, and applied magnetic field.

#### A. Polarization dependence with respect to the sample thickness

As shown in Fig. 4, the polarization measured in the ferromagnetic phase of the reentrant alloys strongly decreases with increasing the sample thickness  $d$ . The effect of the sample thickness is observed at all temperatures below  $T_c$  in the weakly frustrated  $x=0.235$  alloy [Fig. 4(a)]. In the low-temperature state of the  $x=0.30$  alloy [Fig. 4(b)], the polarization returns towards one but a slight influence of the sample thickness remains visible in the value of the flipping ratio. By plotting the polarization in logarithmic scale for several thicknesses [inset Figs. 4(a) and 4(b)], we obtain straight lines that encompass the origin. The fact that  $P$  varies with  $e^{-d}$  is justified in the following by considering the formula derived from Eq. (1). Note that no effect of the sample thickness is observed in the  $x=0.41$  sample that is purely spin glass. In the following, most measurements, except those performed on the  $x=0.30$  sample, concern a single amorphous foil: this ensures a very low demagnetization factor ( $N/4\pi=4 \times 10^{-3}$  in the sample plane) and prevents the existence of stray magnetic fields within the foils.

#### B. Polarization dependence with respect to the neutron wavelength

In this section, we mainly consider measurements performed in a low applied field of 7 Oe. The influence of the applied field will be discussed in a following section. We analyze first of all the general features of the polarization below  $T_c$  then focus on the low-temperature regime.

##### 1. The intermediate temperature range

In Fig. 5, the polarization is shown versus the neutron wavelength  $\lambda$  in the  $x=0.07$ , 0.235, and 0.30 samples, for typical field and temperature values. Clearly the  $P(\lambda)$  variations are very different in the three samples. In the  $x=0.07$  sample (nonfrustrated),  $P(\lambda)$  shows an oscillatory behavior that can be well fitted by a simple cosine law. In the  $x=0.235$  sample (weakly frustrated),  $P$  varies like  $e^{-\lambda^2}$  below  $T_c$ . Finally, in the  $x=0.30$  sample,  $P$  shows a rather complex behavior as a function of  $\lambda$  which is somehow intermediate between the  $e^{-\lambda}$  and  $e^{-\lambda^2}$  variation.

In the  $x=0.07$  sample [Fig. 5(a)], the existence of a

cosine law for the  $P(\lambda)$  variation can be easily derived from the general equation (1) by assuming that all the domain have a unique size that is comparable to the sample thickness ( $d/\delta \sim 1$ ). The polarization data have been fitted by the empirical expression:

$$P(\lambda) = c_1 + c_2 \cos(c_3 \lambda + c_4) \quad (2)$$

By comparing Eq. (2) to Eq. (1) we notice that  $c_1$  corresponds to the mean induction over the sample

( $c_1 = 1 - \langle B_x^2 + B_y^2 \rangle / B^2$ ); the inverse period of oscillation  $c_3$  is related to the domain size  $\delta$  ( $c_3 = \langle cB\delta \rangle$ ). From Eq. (1) the amplitude of oscillations  $c_2$  should be equal to  $1 - c_1$  and the phase term  $c_4$  should be zero, to verify the limiting condition  $P(\lambda=0) = 1$ . The addition of a  $c_4$  term in the cosine law allows to take into account possible phase shifts related to the fact that the polarization vector inclines against the external field axis, due to stray fields from the sample. A fit of the polarization data for

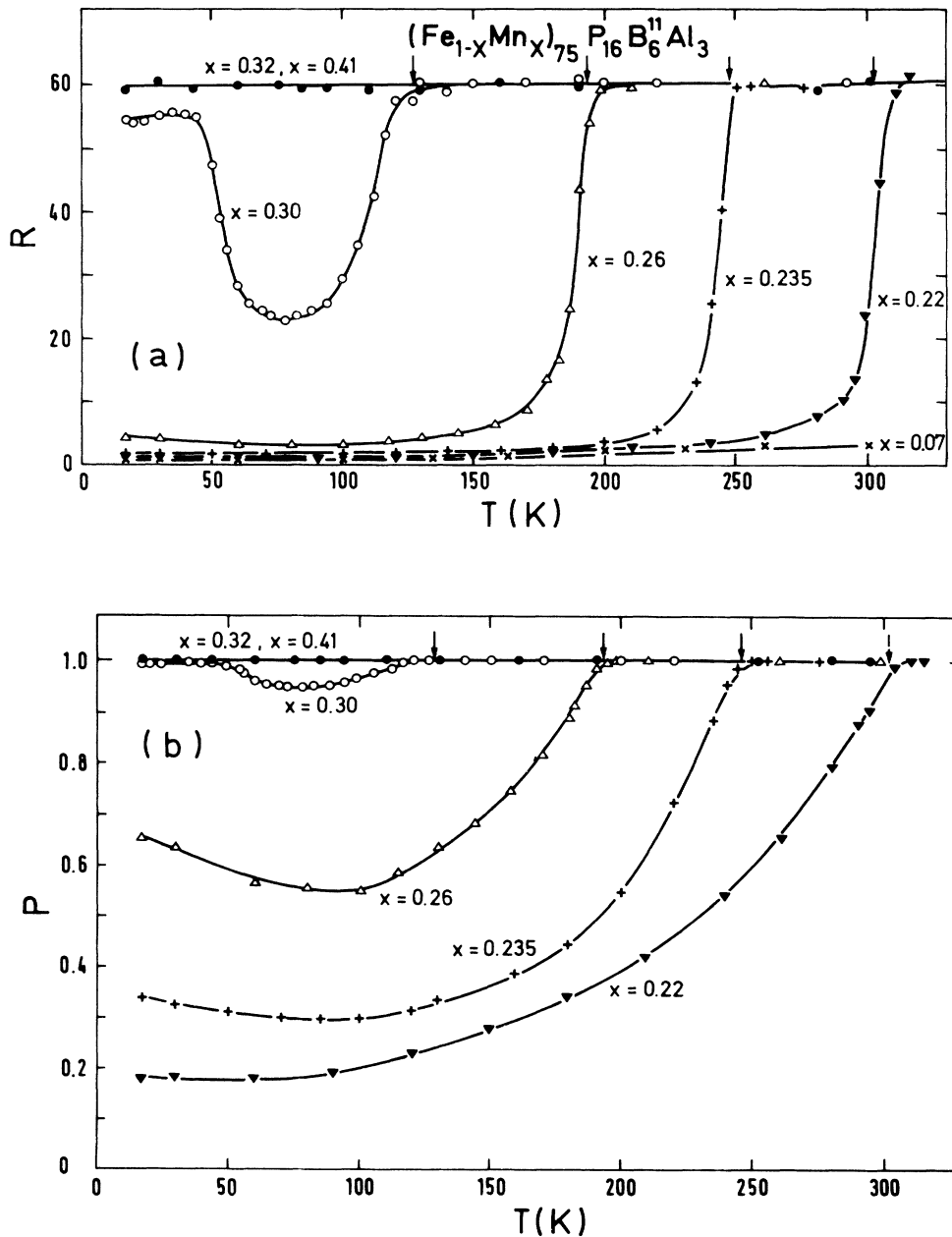


FIG. 3. Flipping ratio  $R$  [Fig. 3(a)] and polarization  $P$  [Fig. 3(b)] as a function of temperature in the  $a\text{-Fe}_{1-x}\text{Mn}_x$  system. These measurements were performed on the spectrometer PADA, with single foils of the amorphous samples ( $25 < d < 70 \mu\text{m}$ ). The neutron wavelength was  $\lambda = 5 \text{ \AA}$  and the applied magnetic field  $H = 5 \text{ Oe}$ . The measurements correspond to a field-cooled state (see the following). The arrows indicate the Curie temperatures.

the lowest field of 7 Oe yields the values (0.379, 0.1097, 1.279, and  $-0.256$ ) for the parameters  $c_1$  to  $c_4$ , respectively. In this low field, the internal field  $B$  in a domain is well approached by the saturated magnetization ( $B \approx 8900$  emu/cm<sup>3</sup> at 289 K). From the value of  $B$  and  $c_3$  we deduce  $\delta \sim 31$   $\mu\text{m}$ , a value close to that of the sample thickness  $d = 35$   $\mu\text{m}$ .

In the  $x = 0.235$  sample [Fig. 5(b)], as well as in the other weakly frustrated alloys ( $0.22 < x < 0.26$ ), the Gaussian variation of the polarization with  $\lambda$  can be well explained by the existence of "small" domains within which the neutron spins precess only a part of their Larmor precession. As shown in Ref. 14, in the limiting case  $cB\delta\lambda \ll 2\pi$ , the general expression is then well approximated by

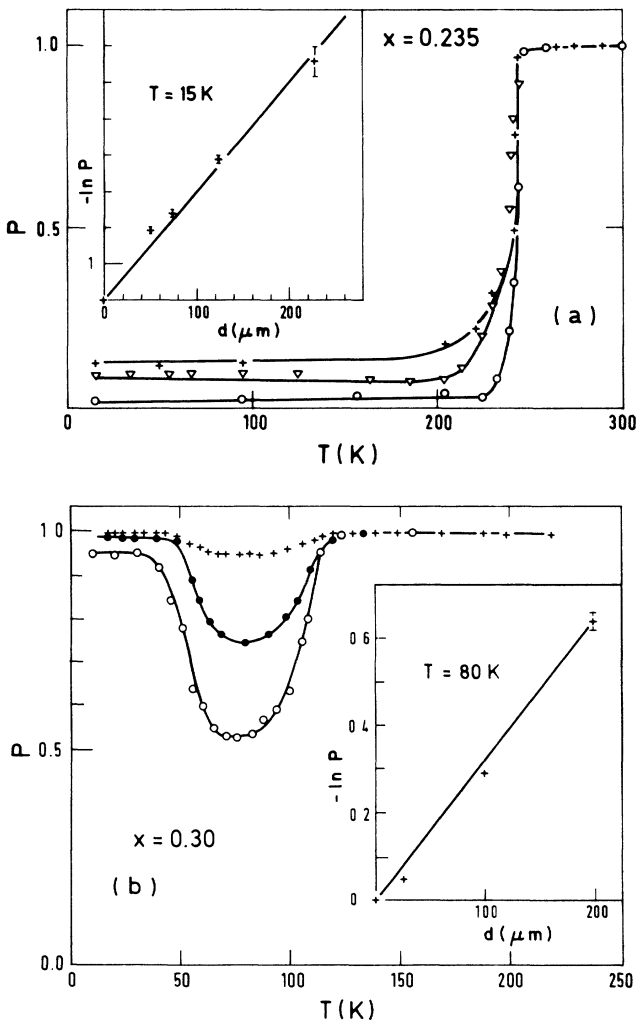


FIG. 4. Polarization dependence with the sample thickness. (a) In the weakly frustrated  $x = 0.235$  sample. Polarization vs temperature for several sample thicknesses  $d$  ( $d = 50$  (+),  $75$  ( $\nabla$ ),  $125$   $\mu\text{m}$  ( $\circ$ )). The measurements are performed on the spin-echo machine with  $\lambda = 7$   $\text{\AA}$ , in a zero applied field. Inset: Logarithm of the polarization measured at low-temperature versus  $d$ . (b) In a strongly frustrated  $x = 0.30$  sample. Polarization vs  $T$  for  $d = 25$  (+),  $100$  ( $\bullet$ ), and  $200$   $\mu\text{m}$  ( $\circ$ ). Inset: Logarithm of the polarization measured at 80 K vs  $d$ .

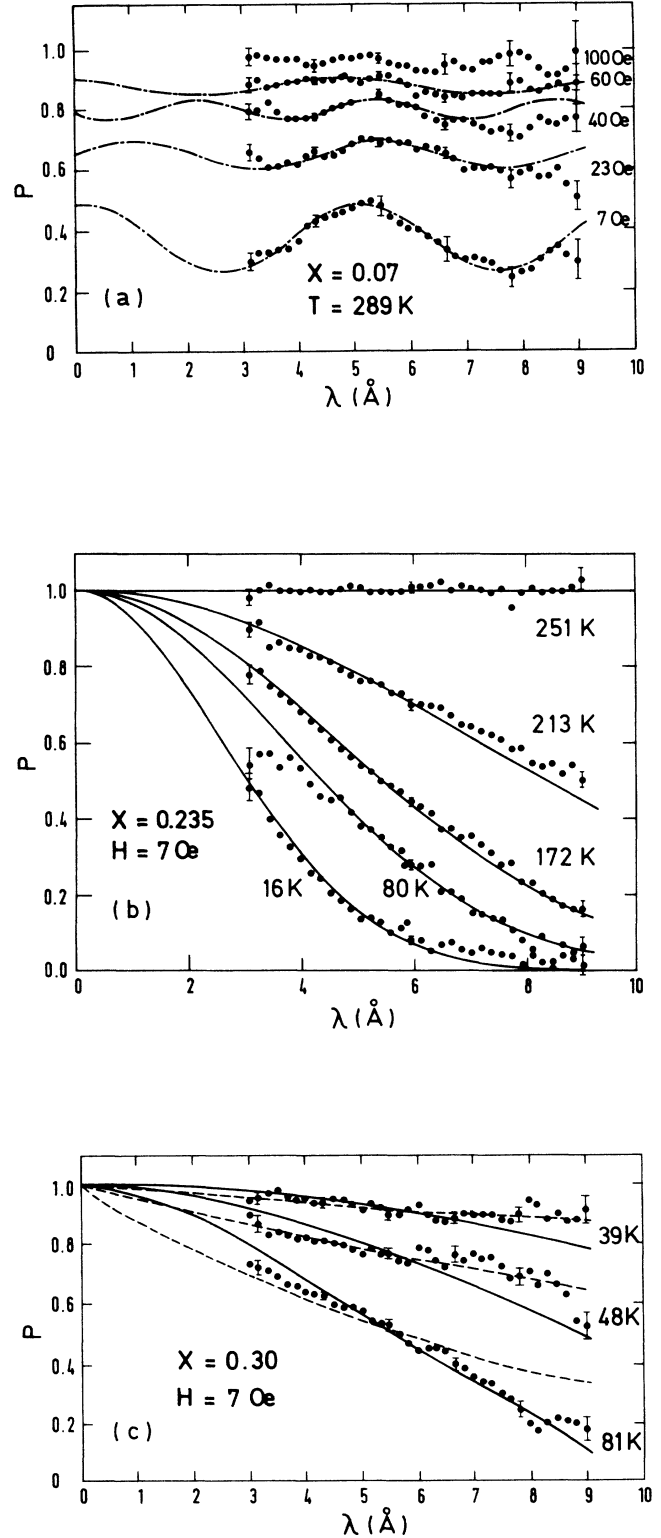


FIG. 5. Polarization dependence with neutron wavelength  $\lambda$ . The polarization has measured on the spectrometer TOP for several applied fields and several temperatures below  $T_c$  in the (a)  $x = 0.07$ , (b)  $x = 0.235$ , and (c)  $x = 0.30$ . Measurements refer to the zero-field-cooled state. The lines are fits to the data according to a cosine law (dotted line), an exponential law (dashed line), or a Gaussian law (solid line) (see the text).

$$P(\lambda) \sim (1 - \frac{1}{2}c^2 \langle B_x^2 + B_y^2 \rangle \delta^2 \lambda^2)^{d/\delta}, \quad (3)$$

which is the first-order term of a Gaussian law

$$P = e^{-\alpha \lambda^2}. \quad (4)$$

In expression (4) the parameter  $\alpha$  is equal to  $\frac{1}{3}c^2 B^2 d \delta$  in case of complete random domain orientation ( $\langle B_x^2 + B_y^2 \rangle = \frac{2}{3}B^2$ ). Here we expect that in a low applied field, the domain will be almost randomly distributed in the sample plane  $yz$  due to demagnetization effects ( $N_y \approx N_z \ll N_x$ ). In this latter case,  $\alpha$  is equal to  $\frac{1}{4}c^2 B^2 d \delta$  since  $B_x = 0$  and  $\langle B_y^2 \rangle = \frac{1}{2}B^2$ .

As shown in the next paragraph, by fitting the data with Eq. (4) and comparing the  $\alpha(T)$  variation to that of the squared magnetization, we evaluate a typical domain size  $\delta$  of about  $5 \mu\text{m}$  in the  $x=0.235$  sample and in the other weakly frustrated alloys ( $0.22 < x < 0.26$ ). We note that this size is still that of a macroscopic scale but is smaller than that measured in the nonfrustrated  $x=0.7$  sample.

In the strongly frustrated  $x=0.30$  sample [Fig. 5(c)], some discrepancy appears when fitting the data by a Gaussian law. This occurs even in the ferromagnetic phase (see the curve for  $T=82 \text{ K}$ ), which suggests that there is no simple domain structure when approaching the critical concentration, as discussed in the conclusion. However, we cannot be sure that this observation is intrinsically related to the frustration. In this sample, the  $P(\lambda)$  variation might have been somehow changed due to the influence of stray fields within the sample foils, since here, eight foils had to be piled up in order to obtain a measurable depolarization signal on the TOP spectrometer.

## 2. The low-temperature regime

At low temperatures, the polarization of the weakly frustrated alloys still obeys a Gaussian dependence with  $\lambda$  but shows some irreversibilities depending on the cooling conditions. We shall now describe in more detail the measurements performed in the  $x=0.235$  sample. Very similar results are observed for  $x=0.26$ .

The influence of the cooling process on the depolarization measured in very low field has been evidenced by two experiments. In the first one we have measured the polarization when cooling the sample either in zero field (ZFC state) or in the 7-Oe field of measurement (FC state). As shown in Fig. 6(a) the ZFC and FC curves separate from each other below about 90 K. In the lowest-temperature range ( $T < 30 \text{ K}$ ), we observe a strong decrease of the ZFC polarization and a slight increase of the FC polarization. In the second experiment, the sample was cooled in a 7-Oe field down to a temperature  $T_0$ , then the field was cut off, while the sample was cooled down to the lowest temperature (11 K) and, finally, the polarization was measured in a 7-Oe field at 11 K. The polarization measured at 11 K is plotted versus  $T_0$  in Fig. 6(b). Above the  $T_0$  value of 90 K,  $P$  is close to its value measured at 11 K in the ZFC state. Upon further decreasing  $T_0$ ,  $P$  increases and becomes close to its value

measured at 11 K in the FC state. Below a  $T_0$  value of about 30 K,  $P$  remains roughly independent of  $T_0$ . Both experiments suggest the existence of two "transitions" below  $T_c$ : one around 90 K, the other one at a lower temperature.

As already shown, the  $P(\lambda)$  variation in a low field of 7 Oe obeys a Gaussian law ( $e^{-\alpha \lambda^2}$ ) in the whole temperature range below  $T_c$ . This observation could be checked whatever the cooling process. In Fig. 7(a) we have reported the temperature dependence of  $\alpha$ , deduced from the measurements of Fig. 6(a), in comparison with that of the square of the technically saturated magnetization  $M^2(T)$ . Above 90 K  $\alpha$  is proportional to  $M^2(T)$ . Below 90 K,  $M^2(T)$  remains roughly constant, whereas some irreversibilities appear in the  $\alpha(T)$  variation, depending on the cooling process.

We note that, in the same  $x=0.235$  sample, small-angle neutron scattering measurements (SANS) in the  $q$  range of  $10^{-2} - 10^{-1} \text{ \AA}^{-1}$  have shown a sharp increase of

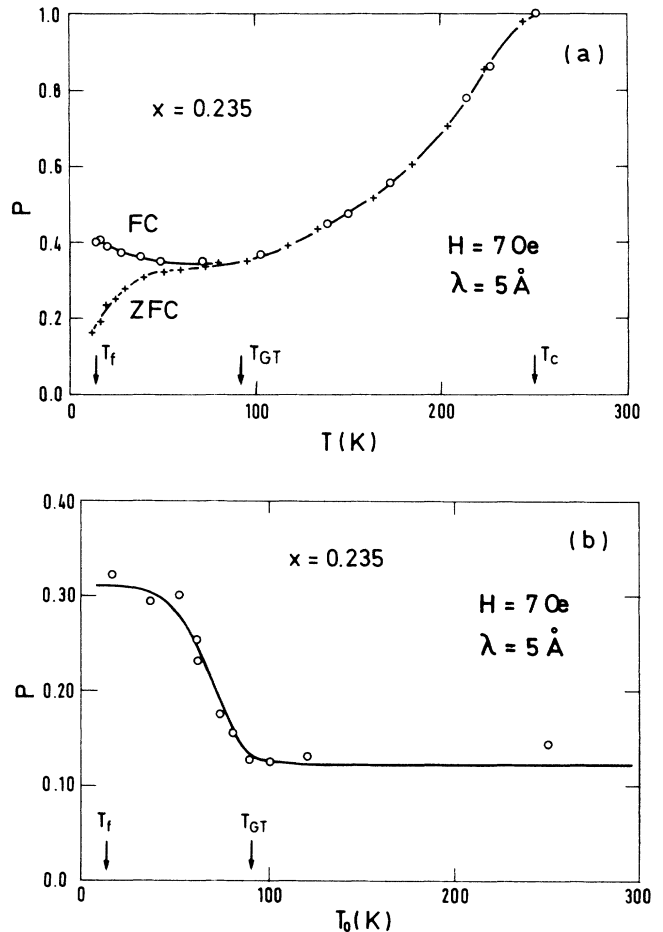


FIG. 6. Influence of the field cooling on the polarization. (a) Irreversibilities of the depolarization in low applied field ( $H=7 \text{ Oe}$ ) in a  $x=0.235$  sample ( $d=60 \mu\text{m}$ ). The polarization is measured as a function of temperature  $T$  for the wavelength  $\lambda=5 \text{ \AA}$ . ZFC (+) and FC (o) refer respectively to the zero-field-cooled and field-cooled state. (b) Polarizability measured at 15 K in 7 Oe as a function of temperature  $T_0$ . The sample has been cooled in a 7-Oe field down to  $T_0$ , then cooled in zero field down to 11 K.

the SANS intensity below 90 K.<sup>15</sup> This signal could be attributed to the freezing of transverse spin components thanks to measurements in applied field.<sup>22</sup> Below this temperature, weak irreversibilities begin to occur in the low-field magnetization (Fig. 1). Thus the temperature  $T_{GT}$  of 90 K, which can correspond to the Gabay-Toulouse transition from a ferromagnetic to a canted state at a microscopic scale ( $\ll 100$  Å), also locates the occurrence of irreversibilities in the domain motion.

Accordingly, we interpret the depolarization results of Fig. 7(a) and 8(a) in the following way. In a low applied field of 7 Oe, the total internal field within the sample is zero, and the internal field within a domain is well approached by the magnetization measured at the limit of the technical saturation plateau ( $B \simeq 4\pi aM$  where  $a$  is the sample density of 5 g/cm<sup>3</sup> and  $M$  the magnetization in an applied field of about 2 kOe). According to Eq. (2) ( $\alpha = \frac{1}{4}c^2B^2d\delta$ ), the fact that  $\alpha(T)$  and  $M^2(T)$  above 90 K are proportional shows that the domain size  $\delta$  remains constant in all the ferromagnetic phase and that the decrease of polarization simply corresponds to the thermal

increase of the longitudinal spin component. From these results we can evaluate a  $\delta$  value of about 5  $\mu$ m in the ferromagnetic phase ( $T > T_{GT}$ ). Below  $T_{GT}$ , the longitudinal magnetization within a domain no more increases ( $M$  becomes independent of  $T$ ), but spin canting occurs, associated with a further increase of the total spin length. Concomitantly, the spin canting induces an anisotropy of the Dzyaloshinsky-Moriya type which reduces the domain wall mobility, leading to irreversibilities in the polarization. These irreversibilities become very strong in the lowest-temperature range ( $T \sim 30$  K). We note that we observe in the same sample a sharp increase of the coercive field below about 25 K. The freezing temperature ( $T_f \simeq 12$  K) determined from the low-field magnetization data is slightly lower. We think that all these features reflect the same physical phenomenon, namely a more complete freezing of the Bloch walls, but illustrate also the difficulty in determining a unique freezing temperature from different macroscopic measurements.

Considering the shape of the ZFC and FC curves of Fig. 6(a), we assume that in a 7-Oe field, a perfect random domain orientation is only obtained when the domains are frozen below 11 K in the ZFC state. When increasing  $T$  from 11 K in the ZFC state, the domains slightly rearrange on the direction of the 7-Oe field, leading to an increase of the polarization. Similarly, the increase of the polarization in the FC state can be explained by slight reorientations during the field cooling. Thus in the case of the weakly frustrated  $x = 0.235$  and  $x = 0.26$  samples, we interpret the low-temperature irreversibilities of the polarization, by some modification of the domain configuration but not of the domain size or magnetization. To support this interpretation, we note that in the same alloys the polarization measured at large wavelength in a zero applied field is almost temperature independent in the low-temperature range [see Fig. 4(a) and Ref. 6].

We insist on the fact that in order to determine the domain size from the depolarization measurements performed in a 7-Oe field, we have used the magnetization measured at the onset of technical saturation, namely in a 2-kOe field, and not the low-field magnetization. This latter quantity does not reflect the internal induction within a domain since it is influenced by dipolar effects and domain wall blocking. In the low frustrated samples, a 2-kOe field mainly aligns the domain walls but does not significantly alter the internal magnetization within a domain with respect to its value in zero field.<sup>15,22</sup>

The situation is rather different in the  $x = 0.30$  sample. As shown in Fig. 2, the technical saturation plateau in the magnetization curve is not well defined and the  $M^2(T)$  variation in a 2-kOe field is smeared around  $T_c$  compared to the  $\alpha(T)$  variation. Clearly, in this sample, the 2-kOe field does not only suppress the domain walls, but it also tends to align the spins in a more microscopic way. These results suggest that there are no well-defined domains and Bloch walls in this case and thus that we cannot determine the domain size and magnetization separately. The most important result remains the decrease of the mean-field integral  $B^2(T)\delta(T)$  at low temperature. By assuming that the main phenomenon is due to the de-

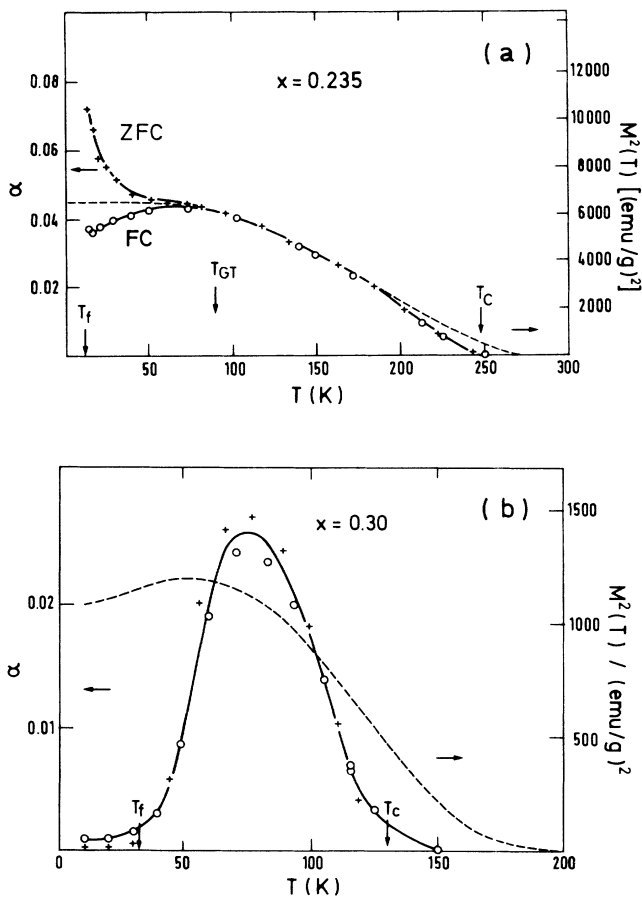


FIG. 7. Temperature dependence of the parameter  $\alpha$  in a  $x = 0.235$  [Fig. 7(a)] and  $x = 0.30$  [Fig. 7(b)] sample.  $\alpha$  is obtained by a fit of the polarization with a Gaussian law  $e^{-\alpha\lambda^2}$  (see the text). ZFC (+) and FC (o) refer respectively to the zero-field-cooled and field-cooled state. Dashed line: Magnetization measured in a field  $H$  of 2 kOe vs temperature.



crease of  $\delta(T)$ , a very schematic picture can be given. Below  $T_c$  an imperfect ferromagnetic order settles in, with no clear distinction between the Bloch walls and the domains. The typical correlation length  $\delta$  is about  $1 \mu\text{m}$ . When lowering the temperature,  $\delta$  decreases. Below about 60 K, the decrease of  $\delta$  overcomes the thermal increase of the magnetization, leading to an increase of the polarization. A residual depolarization remains at low temperature [Fig. 4(b)], which shows that the low-temperature state still keeps some rather long-range correlations ( $\delta \sim 2000 \text{ \AA}$ ). Another explanation of the observed experimental results would also involve a decrease of the domain magnetization at low temperature.

### C. Polarization dependence with the applied field

In this section, we briefly summarize the behavior of the polarization with increase in the applied field above 7 Oe. In all samples, the polarization increases with increasing applied field  $H$  and becomes close to unity when  $H$  becomes greater than a hundred Oe. This effect simply corresponds to a reorientation of the domains along the field axis. Above 100 Oe, the residual depolarization is wavelength independent, which shows the presence of large domains in which the neutron spins make many precessions. Note that this latter case can be derived from the general expression (1) in the limiting case  $cB\delta\lambda \gg 2\pi$ .

In the  $x=0.07$  sample [Fig. 5(a)], the increase of the average polarization occurs concomitantly with a decrease of the amplitude of the oscillations  $c_2$  which can be qualitatively understood by a decrease of the component of the induction  $B_y$  perpendicular to the field. The frequency of oscillations  $c_3$  increases since the domain size  $\delta$  increases.

In the  $x=0.235$  and  $x=0.26$  samples (Fig. 8), the  $e^{-\lambda^2}$  variation is no more obeyed above 7 Oe and  $P(\lambda)$  can be approached by a phenomenological law  $e^{-\beta\lambda}$  with  $\beta$  strongly decreasing with increasing field [Inset Fig. 8(a)]. The influence of field cooling is not observed above 7 Oe. However, the freezing of the domain motion due to the canting can be evidenced above 7 Oe by some hysteresis in the polarization. As shown in the inset of Fig. 8(a), when decreasing applied field from 125 Oe at low temperature, a large hysteresis appears in the polarization value. This hysteresis disappears when approaching the Gabay-Toulouse transition [Inset Fig. 8(b)].

In the  $x=0.30$  sample, the increase of the applied field induces damped oscillations that cannot be fitted by any simple law [Fig. 8(c)]. The damping could be related to a distribution of the correlation lengths as shown in the case of FeAl.<sup>17</sup>

### D. Time-dependent effects

We have performed a few experiments to test the viscosity of the domain motion in the irreversibility region of the  $x=0.26$  sample. The procedure is similar to that used in the case of FeAl.<sup>17</sup> The sample is cooled in the ZFC state at the temperature of measurement and the polarization is measured in a 7-Oe field (state A). Then a

step function magnetic field  $H$  is applied during a time interval  $t_d$  (state B) and finally the polarization is measured during several time intervals in the 7-Oe field (state C). In Fig. 9, we have compared the evolution of the polarization at three temperatures within the same experimental conditions ( $H=125$  Oe,  $t_d=5$  min). At 80-K, state A and C are almost identical, which means that the domain

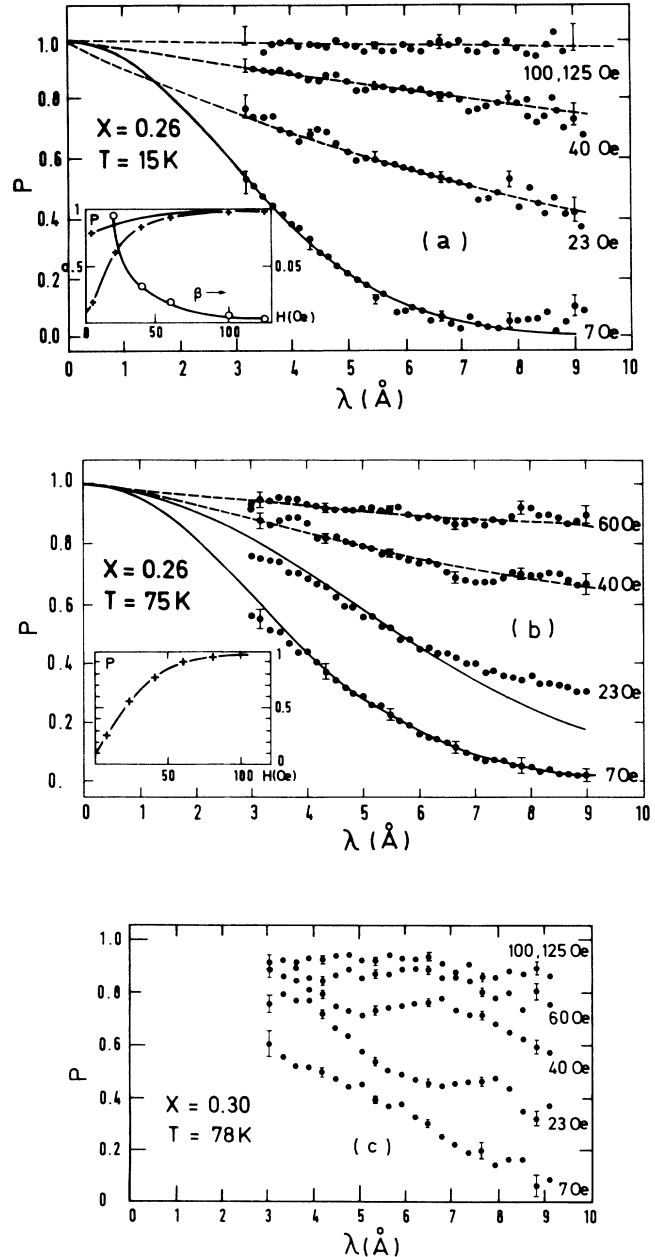


FIG. 8. Polarization dependence with the neutron wavelength for various applied fields  $H$ . (a) in the  $x=0.26$  sample at 15 K. (b) in the  $x=0.26$  sample at 75 K. (c) in the  $x=0.30$  sample at 78 K. In (a) and (b), the lines are fits to the data with a Gaussian law  $e^{-\alpha\lambda^2}$  (solid line) or with an exponential law  $e^{-\beta\lambda}$  (dashed line). Inset of Fig. 8(a) and 8(b): Polarization measured at  $\lambda=5 \text{ \AA}$  and the parameter  $\beta$  deduced from the fit as a function of  $H$ . Note the large hysteresis of the polarization in 8(a).

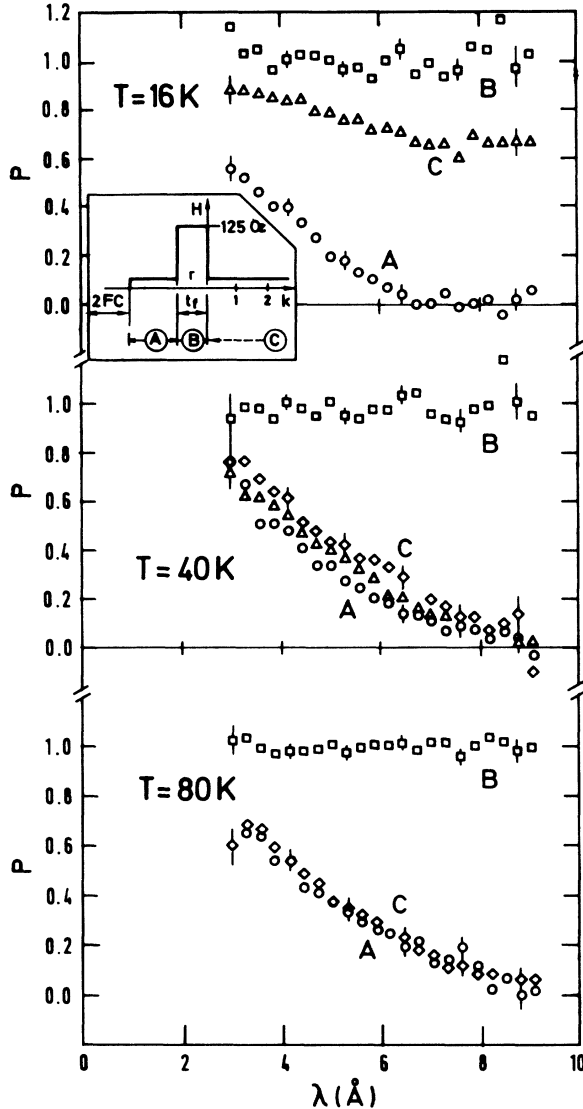


FIG. 9. Time dependence of the polarization in  $a$ -FeMn. Polarization vs the wavelength  $\lambda$  at several temperatures in the state  $A$  ( $\circ$ ),  $B$  ( $\square$ ), and  $C$  described in text. In state  $C$ , the polarization has been measured in the time intervals  $0 < t < 5$  min ( $\diamond$ ),  $10 < t < 20$  min ( $\triangle$ ), and  $150 < t < 180$  min (same results as for  $\triangle$ ).

structure follows the changes of applied field immediately. At 40 K, state  $C$  relaxes towards state  $A$  within a few hours. Finally at 16 K, the relaxation is so slow that it could not be observed within the time of experiment. The results clearly show that the strong increase of the coercivity observed at low temperature in the magnetization is related to a freezing in the domain motion.

## V. CONCLUSION

We have measured the depolarization in a reentrant system  $a$ -Fe $_{1-x}$ Mn $_x$  by varying the concentration  $x$  from the case of the conventional ferromagnetic ( $x=0.07$ ) to that of a true spin glass ( $x=0.41$ ). By checking the influence on the depolarization of several important parameters like the sample thickness, the neutron wave-

length, and the applied magnetic field, we can deduce a typical domain size  $\delta$  in a very low or zero magnetic field, which corresponds to the scale of the longitudinal correlations. The  $\delta$  values are reported in Table I as a function of  $x$ . In the nonfrustrated sample ( $x=0.7$ ), the polarization oscillates with  $\lambda$  with a simple cosine law, which means that the domain size is rather large and comparable to the sample thickness ( $\delta \sim 31 \mu\text{m}$ ). In the reentrant alloys  $\delta$  is strongly reduced. Interestingly enough, although the susceptibility and low-field magnetization exhibit a rather unique behavior with temperature for all the reentrant alloys (the well-known bell shape), we observe qualitative differences in the polarization, depending on the amount of frustration. In the weakly frustrated samples ( $0.22 < x < 0.26$ ) the polarization varies like  $e^{-\lambda^2}$ , which can be interpreted by the existence of domains of about  $4\text{--}6 \mu\text{m}$ . This domain size does not change with temperature down to the lowest temperature as shown by measurements in zero field. Irreversibilities of the polarization at low field and low temperature are interpreted by a blocking of the domain motion due to the occurrence of the canted state, rather than by a change of the domain size. By contrast, in the strongly frustrated  $x=0.30$  sample, the sharp minimum of the  $P(T)$  curve indicates a decrease of either the domain size or magnetization with temperature. Most probably an imperfect ferromagnetic order settles in, with no clear distinction between the domains and the Bloch walls, so that both phenomena would occur together. By assuming that the  $\delta$  variation is predominant, we obtain a typical  $\delta$  size of about  $1 \mu\text{m}$  below  $T_c$ , decreasing to about  $2000 \text{ \AA}$  at low temperature. Finally, in the  $x=0.32$  sample which is close to the critical point of the phase diagram, no depolarization is observed as in the true spin glass  $x=0.41$  which shows that  $\delta$  is smaller than  $2000 \text{ \AA}$ .

In ferromagnets, the size of the domains mainly results from a competition between the exchange and dipolar energies. We can therefore understand the observed decrease of the domain size with Mn concentration as a result of the decrease of the magnetization. In the weakly frustrated reentrant spin glasses, the typical domain size  $\delta \approx 5 \mu\text{m}$  is in good agreement with that measured by electron microscopy.<sup>8</sup> The persistence of domains at low temperature associated with a strong depolarization in

TABLE I. Typical domain size  $\delta$  in  $\mu\text{m}$  as a function of concentration  $x$  in the  $a$ -Fe $_{1-x}$ Mn $_x$  system.  $\delta$  is deduced from the low-field depolarization data ( $0 \leq H \leq 7 \text{ Oe}$ ). The typical sample thickness  $d$  in  $\mu\text{m}$  is also quoted.

$x$	$\delta(\mu\text{m})$	$d(\mu\text{m})$
0.07	31	35
0.22	4	70
0.235	7	45
0.247	6	44
0.26	5	45
0.30	1.7 <sup>a</sup>	25
0.32	<0.2	25
0.41	<0.2	50

<sup>a</sup>Decreasing to about  $2000 \text{ \AA}$  at low  $T$ .

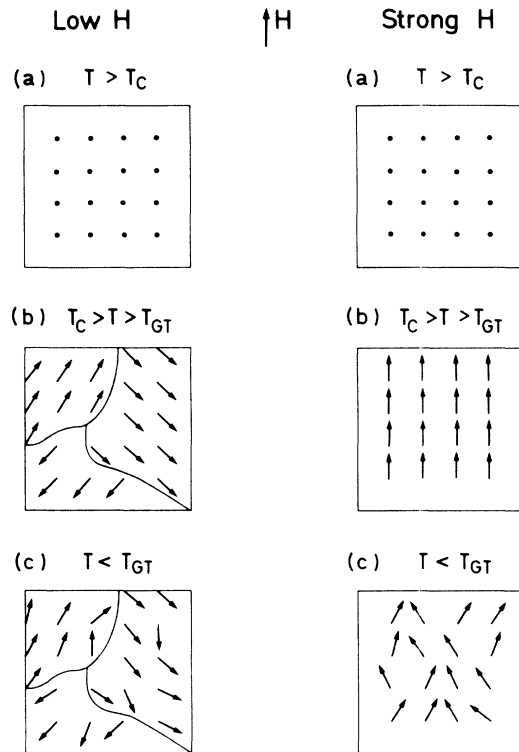


FIG. 10. Schematic picture of the domain configuration in a weakly reentrant alloy. The system is shown either under a low applied field  $H$  of zero to a few Oe (left part of the figure) or under a strong field of a few kOe, which aligns the domains but does not suppress the canted state (right part of the figure). When decreasing the temperature, we observe the following: (a) the paramagnetic state  $T > T_c$ , (b) the ferromagnetic state  $T_c > T > T_{GT}$ , and (c) the canted ferromagnetic state  $T < T_{GT}$ . At low temperature,  $T < T_f < T_{GT}$ , the domain configuration looks basically the same, but strong irreversibilities occur in the domain motion. Note that a very strong field ( $H \sim 200$  kOe) would be necessary to suppress the canting (Refs. 15 and 21).

zero applied field [Fig. 4(a)], confirms the predictions of the classical mean-field model of Gabay and Toulouse<sup>2</sup> with infinite range of interactions. By contrast, the behavior of the  $x=0.30$  sample, shows that when approaching the critical concentration, short-range interactions become dominant so that the frustration induces a decrease of the domain size or internal magnetization at low temperature. This reveals the limits of the classical MF theory near the percolation threshold. A decrease of the domain size is indeed predicted by the random-field

approach. However, in all cases, the  $\delta$  size which is nearly macroscopic (from  $5 \mu\text{m}$  to about  $2000 \text{ \AA}$  near the critical point) is much greater than the typical correlation length deduced from SANS experiments<sup>4</sup> within the RF model ( $\delta \sim 10 \text{ \AA}$ ). The local mean-field approach recently developed by Saslow and Parker,<sup>3</sup> which predicts not only a canting transition but also a decrease of the internal magnetization at a still lower temperature could be more suitable to our results. Anyway, like in  $\text{EuSrS}$ ,<sup>23</sup> we must admit that the inhomogeneities of rather short scale which are observed by SANS are imbedded in domains of much larger scale. The occurrence of canting modifies not only the microscopic scale studied by SANS, but also the domain motion as revealed by the irreversibilities in the depolarization. Very interestingly, a strong applied field which aligns the domains, does not restore a true ferromagnetic state. Spin canting persists in applied field, associated with static and dynamic anomalies, as shown by SANS and inelastic measurements.<sup>22</sup> A schematic picture of the domain configuration, showing the effect of canting in low and high applied field, is given in Fig. 10.

Recent depolarization measurements performed in amorphous  $\text{FeNi}$  (Ref. 24) and crystalline  $\text{AuFe}$  (Refs. 14 and 25) yield results rather similar to those obtained in  $\alpha\text{-FeMn}$ . In the  $\text{NiMn}$  and  $\text{FeZr}$  systems,<sup>26</sup> the MF approach seems to work even better since we observe no minimum of the polarization versus temperature, even in the samples very close to the critical point. By contrast it appears that the  $\text{FeAl}$  system could be intrinsically different and might obey the RF predictions, as shown both by the depolarization and the spin waves anomalies.

#### ACKNOWLEDGMENTS

Two of the authors (I.M. and M.H.) are much indebted to I. A. Campbell, who initiated their depolarization measurements in reentrant spin glasses and advised them through many discussions. The help of F. Hippert, A. Miedan-Gros, and K. Takada during the magnetization measurements is gratefully acknowledged. For the depolarization measurement we have benefited from the help of P. Calmettes and R. Millet at Orphée and S. M. Shapiro at Brookhaven. We also thank H. Yoshisawa for useful discussions. One of us (I.M.) acknowledges support from the Japan-France collaboration program, the Japanese Society for the Promotion of Science (JSPS) and the Centre National de la Recherche Scientifique (CNRS). The Laboratoire Léon Brillouin is associated with le Commissariat à l'Énergie Atomique (CEA) and with le Centre National de la Recherche Scientifique (CNRS).

<sup>1</sup>D. Sherrington and S. Kirkpatrick, Phys. Rev. Lett. **35**, 1792 (1975); S. Kirkpatrick and D. Sherrington, Phys. Rev. B **17**, 4384 (1978).

<sup>2</sup>M. Gabay and G. Toulouse, Phys. Rev. Lett. **47**, 201 (1981).

<sup>3</sup>W. M. Saslow and G. N. Parker, Phys. Rev. Lett. **56**, 1074 (1986); G. N. Parker and W. N. Saslow, Phys. Rev. B **38**, 11 718 (1988).

<sup>4</sup>G. Aeppli, S. M. Shapiro, R. J. Birgenau, and H. S. Chen, Phys. Rev. B **28**, 5160 (1983); **29**, 2589 (1984).

<sup>5</sup>M. B. Salomon, K. V. Rao, and H. S. Chen, Phys. Rev. Lett. **44**, 596 (1980); Y. Yeshurun, M. B. Salomon, K. V. Rao, and H. S. Chen, Phys. Rev. Lett. **45**, 1366 (1980) and Phys. Rev. B **24**, 1536 (1981); M. A. Manheimer, S. M. Bhagat, and H. S. Chen, Phys. Rev. B **26**, 456 (1982); J. Magn. Magn. Mater. **38**, 147 (1983).

<sup>6</sup>W. Abdul-Razzac and J. S. Kouvel, J. Appl. Phys. **55**, 1623 (1984).

<sup>7</sup>S. Senoussi, J. Phys. **45**, 315 (1984).

- <sup>8</sup>S. Senoussi and Y. Oner, *J. Phys.* **46**, 1435 (1985).
- <sup>9</sup>S. Senoussi, S. Hajoudj, and R. Fourmeaux, *Phys. Rev. Lett.* **61**, 1013 (1988).
- <sup>10</sup>H. Yoshizawa, S. Mitsuda, H. Aruga, and A. Ito, *Phys. Rev. Lett.* **59**, 2364 (1987).
- <sup>11</sup>A. P. Murani, *Solid State Commun.* **304**, 705 (1980); H. Maletta, G. Aeppli, and S. M. Shapiro, *Phys. Rev. Lett.* **48**, 1490 (1982).
- <sup>12</sup>G. Halpern and T. Olstein, *Phys. Rev.* **59**, 960 (1941).
- <sup>13</sup>M. Th. Rekveldt, *Z. Phys.* **259**, 391 (1973).
- <sup>14</sup>S. Mitsuda and Y. Endoh, *J. Phys. Soc. Jpn.* **54**, 1570 (1985).
- <sup>15</sup>I. Mirebeau, G. Jehanno, I. A. Campbell, F. Hippert, B. Hennion, and M. Hennion, *J. Magn. Magn. Mater.* **54**, 99 (1986).
- <sup>16</sup>I. Mirebeau, S. Lequien, M. Hennion, F. Hippert, and A. P. Murani, *Physica B* **156**, 201 (1989).
- <sup>17</sup>S. Mitsuda, Y. Endoh, and H. Yoshizawa (unpublished).
- <sup>18</sup>M. Hennion, I. Mirebeau, B. Hennion, S. Lequien, and F. Hippert, *Europhys. Lett.* **2**, 393 (1986).
- <sup>19</sup>M. Hennion, B. Hennion, I. Mirebeau, S. Lequien, and F. Hippert, *J. Appl. Phys.* **63**, 4071 (1988).
- <sup>20</sup>R. B. Goldfarb, F. R. Fickett, K. V. Rao, and H. S. Chen, *J. Appl. Phys.* **53**, 7687 (1982); R. B. Goldfarb, K. V. Rao, H. S. Chen, and C. E. Patton, *J. Appl. Phys.* **53**, 2217 (1982).
- <sup>21</sup>H. Rakoto, J. C. Ousset, S. Senoussi, and I. A. Campbell, *J. Magn. Magn. Mater.* **46**, 212 (1984).
- <sup>22</sup>M. Hennion, B. Hennion, I. Mirebeau, S. Lequien, and F. Hippert, *J. Phys. (Paris) Colloq.* **C8-12**, 49 (1988); 112 (1988).
- <sup>23</sup>S. Gerschwind, G. Devlin, and S. L. McCall, *Phys. Rev. Lett.* **58**, 1895 (1987).
- <sup>24</sup>R. W. Erwin, *Proceedings of the Conference on Magnetism and Magnetic Materials (MMM)*, Boston, 1989 [*J. Appl. Phys.* (to be published)].
- <sup>25</sup>S. Mitsuda, H. Yoshisawa, I. Mirebeau, S. Itoh, T. Watanabe, and Y. Endoh (unpublished).
- <sup>26</sup>I. Mirebeau, S. Itoh, S. Mitsuda, F. Watanabe, Y. Endoh, M. Hennion, and P. Calmettes, *Proceedings of the Conference on Magnetism and Magnetic Materials (MMM)*, Boston, 1989 [*J. Appl. Phys.* (to be published)].